

## Quantum tunneling of surface-state electrons

S. Yücel and E. Y. Andrei

*Department of Physics and Astronomy, Rutgers University, Piscataway, New Jersey 08855*

(Received 27 February 1990)

We have calculated quasi-bound-state energies and lifetimes of surface-state electrons above liquid helium for two single-particle potentials. In the first case, the electric field due to other electrons is taken to be that of a uniform charge sheet. The second is an effective one-particle potential that includes correlation effects in a simple manner. We solved the Schrödinger equation numerically to determine the asymptotic amplitude and the phase of the wave function, from which resonances and their widths are obtained. Tunneling rates and thermal activation energies are calculated as a function of correlation-hole radius, electron density, and pressing electric field amplitude. We compare these results with recent experiments.

### INTRODUCTION

Tunneling of a particle through a potential barrier is a standard topic in quantum mechanics. But when the tunneling particle is coupled to an external environment the picture changes drastically. In recent years work on this problem has been stimulated by new developments in microstructures and devices such as the Josephson junctions,<sup>1</sup> the tunneling electron microscope,<sup>2</sup> and the resonant tunneling diode.<sup>3</sup> The system of surface-state electrons above liquid helium is particularly suited for a systematic study of the effect of interactions on a tunneling electron. This is a quasi-two-dimensional (2D) layer of electrons that can be made to tunnel through an externally adjustable barrier. The tunneling electron couples to the environment via well-known electron-electron and electron-rippion interactions, both of which are experimentally adjustable over a wide range of parameters.

An electron above liquid helium is attracted to it by an image charge<sup>4</sup> but at the surface it is prevented from penetrating the liquid by a 1-eV repulsive barrier. If this barrier is made infinitely high, then in the perpendicular direction  $z$ , the potential is that of a one-dimensional hydrogen atom with a scaled nuclear charge  $Z = (\epsilon - 1)/4(\epsilon + 1)$ , where  $\epsilon = 1.0572$  is the dielectric constant of the liquid helium. Solving the Schrödinger equation for this weakly bound hydrogen atom in atomic units, scaled to take into account the reduced charge, results in the usual Rydberg series of bound-state energies and the corresponding radial wave functions.<sup>4,5</sup> The small scale of the resulting binding energies 1 meV  $\ll$  1 eV, justifies the infinite-barrier approximation. In the ground state the wave function describes an electron free to move in a plane parallel to the liquid helium surface at a distance of 114 Å above it.

When many electrons are present, as is the case in most experiments, they form a 2D layer of interacting charges. Far above the surface, at large distances compared to the interelectronic spacing  $a$ , this charge layer looks uniform and the potential seen by an electron acquires a repulsive contribution arising from the field of the uniform charge sheet  $\mathcal{E}_c = 2\pi ne$ , where  $n$  and  $e$  are the electron surface

density and the magnitude of the electron charge, respectively. The total potential seen by the electron for large  $z$  is thus  $U(z) \approx -1/z - \mathcal{E}_c z$ . We expressed the potential in scaled atomic units (s.a.u.),<sup>6</sup> which we will be using for the rest of this paper. This potential allows electrons to escape from the surface by tunneling. To prevent their escape, the electrons are confined vertically with a pressing field  $\mathcal{E}_p \geq \mathcal{E}_c$  created between two parallel plates. At zero temperature, if the potential between the metal plates is reduced so that  $\mathcal{E}_p < \mathcal{E}_c$ , the electrons can escape from the liquid helium surface by tunneling from the ground state. At finite temperatures, the total escape rate will have contributions from thermally activated escape as well as from tunneling out of excited states.

Near the surface the details of the charge distribution and the interactions with the tunneling electron will result in a more complicated potential. Thus, escape from the surface can no longer be viewed as a single-particle problem and correlations between electrons need to be included in any calculation of tunneling rates and thermal activation energies. The strength of correlations between the electrons is determined by the ratio of electronic potential energy to thermal energy:  $\Gamma = (\pi n)^{1/2} e^2 / kT$ , where  $T$  is the electronic temperature. When  $\Gamma \geq 50$ , the electrons are localized within a correlation radius  $r_0 \approx (\pi n)^{-1/2}$  about their equilibrium positions.

The effects of correlations on the activation energies were first demonstrated by Iye *et al.*<sup>7</sup> who also introduced a simple model to take them into account. According to this model, at sufficiently high densities and low temperatures, each electron excludes all neighboring electrons from a disk of radius  $r_0$  around it. As the electron moves out of the surface, the correlation hole shrinks and closes at a distance  $z = r_0$ . This simple effective one-particle potential approach gives good estimates for the thermal activation energies in the presence of correlations. This was also illustrated in a recent paper by Goodkind *et al.*<sup>8</sup> who measured escape rates and the thermal activation energies of electrons in the density regime of  $n = 3 \times 10^7 - 5 \times 10^8 \text{ cm}^{-2}$ , where correlation effects are significant. The measured thermal activation energies were in good agreement with calculations using

the correlation-hole model of Iye *et al.* This suggests the possibility of applying the same model to calculations of tunneling rates. To observe tunneling, Goodkind *et al.* monitored the temperature dependence of the escape rates. At around 0.5 K, the escape rates became temperature independent, and Goodkind *et al.* identified them as tunneling rates out of the ground state. But the measured rates turned out to be many orders of magnitude larger than those expected from a WKB calculation of the tunneling rates.

#### METHODS FOR CALCULATING TUNNELING RATES

To estimate the tunneling rates Goodkind *et al.* multiplied the transmission probability of a free particle through this barrier, by an attempt frequency that is taken to be  $E_1/(2\hbar)$ , where  $E_1$  is the ground-state energy. Even though an electron above the liquid helium has a continuous spectrum, the physically interesting states are the quasi-bound-states or resonances which can be characterized by a quasi-bound-state energy  $E_r$  and an associated width  $W$ . Since, on the liquid helium side of the barrier, resonances look more like bound states rather than a state that asymptotically becomes a plane wave, such an oversimplification is difficult to justify. A proper calculation of tunneling rates by the WKB approximation requires knowledge of both the wave function near the origin and a good estimate for  $E_r$ . After calculating the wave function by WKB method and then matching to the solution around the origin, the tunneling rates can be determined from the probability current at resonant energy.

In the absence of correlations the problem reduces to that of a 1D hydrogen atom in an external electric field, the "Stark effect." Reasonable estimates for the resonance energies can be obtained in this case by using first-order perturbation theory. Nevertheless, for more complicated potentials that include correlation effects, a perturbative approach needs to be justified. There are several methods which can be used to calculate resonance energies and lifetimes essentially exactly. Resonances can be described by the phase shift of the asymptotic form of the wave function or by the poles of the scattering amplitudes,<sup>9,10</sup> in which case they can be deduced from the asymptotic solution of the wave function. Alternatively, they can be described as poles of the resolvent operator and obtained by directly solving a complex scaled Hamiltonian that has identifiable complex eigenvalues corresponding to these resonant states.<sup>11</sup> Both methods have been successfully applied in the past to the 3D hydrogen atom.

In this paper we calculate tunneling rates and resonance energies by using the asymptotic form of the wave function, AFW. All the computational and mathematical details are given in the Appendix. In the simpler uncorrelated case, we compared these to calculations employing the complex scaling and the WKB approximation. The advantage of using the AFW approach is the relative ease with which it can be applied not only to the ordinary 1D Stark potential but also to more complicated potentials, for determining resonance energies and life-

times. An additional advantage of this method is the ability to calculate very narrow resonances, which may require a large investment in code development if the complex scaling method is used.

We carried out an accurate and systematic study of tunneling rates and quasi-bound-state energies by using the simple model of Iye *et al.* to account for correlations. Since its general features are shared by other potentials obtained by more sophisticated treatments,<sup>12</sup> it seems sufficient for answering the central question of this paper, that is, whether tunneling is the mechanism responsible for the reported temperature-independent escape rates. We find that the tunneling rates out of the ground state are  $\sim 25$ – $45$  orders of magnitude slower than the observed rates. Either the escape is not due to tunneling from the ground state, or an effective single-particle potential is inadequate to describe the interactions. We conclude this paper by showing that at the temperatures employed in the experiment, tunneling out of excited states should be significant and could completely mask the tunneling out of the ground state. The latter may not be measurable unless the temperature is reduced below 200 mK.

#### RESULTS AND DISCUSSION

In Table I, we tabulated the resonance energies and the lifetimes for the ordinary Stark effect for a one-dimensional hydrogen atom as calculated by the AFW method. As a check, some of the data are also calculated by the complex scaling method that employs the nonorthogonal basis

$$\phi_s(z) = z\sqrt{2(s+1)}e^{-z}F(-s, 2, 2z), \quad (1)$$

where  $F(-s, 2, 2z)$  is a confluent hypergeometric function and  $s=0, 1, 2, \dots$ . The details of the complex scaling calculations and their applications to escape through time-dependent potentials will be given in a forthcoming publication. The agreement between the two methods is excellent at low fields. At higher fields we note small deviations, which is not surprising since the AFW technique is less accurate for the description of broad resonances. As expected, the shifts are accurately given by  $-3\mathcal{E}/2$  which is the first-order correction to the energy.

We now compare these results to the ones obtained with the WKB method. The tunneling rates for the  $1s$  state in the 3D hydrogen atom are well approximated by the WKB formula.<sup>13</sup> A one-dimensional version of this formula was calculated by Geltman,<sup>14</sup>

$$\Gamma = \left[ \frac{2|2E|}{\mathcal{E}} \right]^{2|2E|^{-1/2}} \exp \left[ -\frac{2(|2E|)^{3/2}}{3\mathcal{E}} \right]. \quad (2)$$

When the unperturbed ground-state energy of the electron,  $E_1 = -\frac{1}{2}$ , is used in (2), the resulting rates are roughly an order of magnitude larger than the correct rates, while using the resonance energy  $E_r$  from Table I produces rates that are smaller approximately a factor of 4. Therefore if the constant 2 in the prefactor of (2) is replaced by 4 and  $E_r$  is used, all the rates calculated from this modified Geltman formula, given in Table I, ap-

TABLE I. Resonance energies  $E_r$  and the widths  $W$  for the 1D Stark effect. Also given is the result of the complex scaling method which employs a Sturm basis and the widths obtained from the modified Geltman formula for the lifetimes of a 1D hydrogen atom.  $x[y]=x \times 10^y$ .

Field	AFW		Complex scaling		WKB
	$E_r$	$W$	$E_r$	$W$	$W$
0.050	-0.580 312 4	2.89[-4]	-0.580 316 157	2.9696[-4]	4.96[-4]
0.045	-0.571 579 8	9.00[-5]	-0.571 579 769 8	9.0143[-5]	1.41[-4]
0.040	-0.563 067 240	1.92[-5]	-0.563 067 242 9	1.9215[-5]	2.84[-5]
0.035	-0.554 748 833	2.47[-6]	-0.554 748 833 0	2.4724[-6]	3.46[-6]
0.030	-0.546 591 510 8	1.49[-7]	-0.546 591 510 8	1.4907[-7]	1.98[-7]
0.025	-0.538 569 193 8	2.66[-9]	-0.538 569 193 8	2.660[-9]	3.36[-9]
0.020	-0.530 663 983 5	5.56[-12]			6.69[-12]
0.015	-0.522 863 241 6	1.55[-16]			1.78[-16]
0.010	-0.515 157 301 3	8.16[-26]			8.93[-26]

proach the exact results. It is instructive to note that  $E_r$  rather than the barrier height  $E_r + 2\sqrt{\mathcal{E}}$  needs to be used in (2) to get reasonable rates.

In Table II we list the calculated thermal activation energies  $Q$  in the presence of correlations for the field and density values reported by Goodkind *et al.* They are in reasonable agreement with almost all the data. The agreement is best for high electron densities or small  $r_0$  and worst for the small density or large  $r_0$  for which the calculated values are higher by 1–3 K. In all of these calculations we took  $r_0 = 1.38(\pi n)^{-1/2}$ , which probably overestimates  $r_0$  at low densities and could be the source of this discrepancy.<sup>15,16</sup> We note that if one uses the ground state of a one-dimensional hydrogen atom as the unperturbed state, the calculated shift in energy, from first-order perturbation theory, would be approximately  $-3\mathcal{E}_c/(2r_0) + 3\mathcal{E}_p/2$ . The exact shifts, as in the case of ordinary Stark shifts, are close to the first-order shifts.

This is partly because  $U_c(z)$  contributes very little to the ground-state shifts for large  $r_0$ .

The correlation radius and pressing field dependence of the tunneling rates are plotted in Figs. 1 and 2 for three sets of field and density values. An estimate for the tunneling rates when  $r_0 = 1.38(\pi n)^{-1/2}$  can be obtained by a simple extrapolation. The extrapolated values are in the range  $10^{-45} - 10^{-67}$ , and as expected, are extremely small compared to experimental rates that are all of order  $10^{-18}$ . The discrepancy is more than 25 orders of magnitude for the large density and more than 45 orders of magnitude for the smallest density.

As illustrated in Fig. 3, the calculated tunneling rates could be brought into agreement with the experimental escape rates by reducing the width of the potential barrier. This can be done by reducing the correlation radius by a factor of 2–3. But reducing  $r_0$  would also reduce the height of the barrier causing a discrepancy to appear

TABLE II. Quasi-bound-ground-state energies  $E_r$  and activation energies  $Q$  for the experimentally measured cases. Experimental activation energies  $Q_{\text{expt}}$  are from Ref. 8. The cgs units for  $n$  can be obtained by dividing  $\mathcal{E}_c$  by  $0.0524 \times 10^{-8}$ .

$E_r$	$r_0$	$\mathcal{E}_c$	$\mathcal{E}_p$	$Q$	$Q_{\text{expt}}$
-0.442 124 701 8	92.21	0.0644	0.0406	1.605 01	1.57
-0.442 354 539 0	89.36	0.0686	0.0405	1.491 71	1.51
-0.460 459 825 1	87.05	0.0723	0.0278	0.895 84	0.97
-0.460 076 804 4	89.69	0.0681	0.0280	0.949 24	0.96
-0.457 121 878 4	88.34	0.0702	0.0301	1.000 79	1.04
-0.455 755 176 7	86.74	0.0728	0.0311	1.004 98	0.85
-0.454 721 229 6	87.69	0.0712	0.0318	1.051 91	1.04
-0.451 913 862 4	86.74	0.0728	0.0338	1.107 68	1.10
-0.452 267 655 1	88.67	0.0696	0.0335	1.143 71	1.13
-0.473 620 712 0	134.28	0.0303	0.0181	1.187 09	0.96
-0.478 787 109 5	147.61	0.0251	0.0145	1.085 29	0.94
-0.482 083 040 5	165.90	0.0199	0.0122	1.092 67	0.96
-0.482 396 496 6	159.71	0.0214	0.0120	1.008 57	0.58
-0.470 733 726 2	107.20	0.0476	0.0203	0.912 89	0.69
-0.467 091 185 1	109.02	0.0461	0.0228	1.063 22	1.04
-0.464 136 781 2	104.92	0.0497	0.0249	1.099 55	1.00
-0.474 971 687 9	128.84	0.0330	0.0172	1.037 60	0.78
-0.488 497 853 1	193.26	0.0146	0.0078	0.881 48	0.71

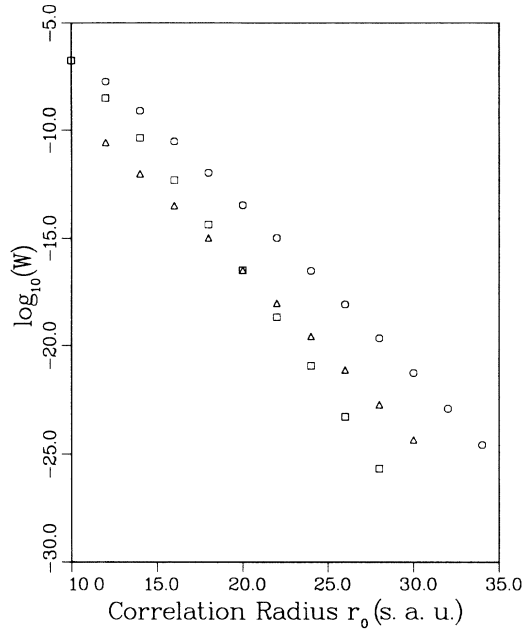


FIG. 1. Correlation radius  $r_0$  dependence of tunneling rates  $W$  from the ground state.  $\mathcal{E}_c$  and  $\mathcal{E}_p$  are ( $\circ$ ) 0.052, 0.143, ( $\square$ ) 0.105, 0.236, ( $\triangle$ ) 0.029, 0.075, respectively. The values for  $r_0 = 1.38 (\pi n)^{-1/2}$  are 62, 48, and 85, respectively.

with the measured thermal activation rates. Alternatively, as seen from Fig. 2 for  $n = 2.7 \times 10^8 \text{ cm}^{-2}$  and  $\mathcal{E}_p = 91 \text{ V/cm}$ , the width of the barrier could be reduced by reducing the external field by more than a factor of 3 while keeping the correlation radius fixed. But again this would substantially reduce the barrier height. Evidently

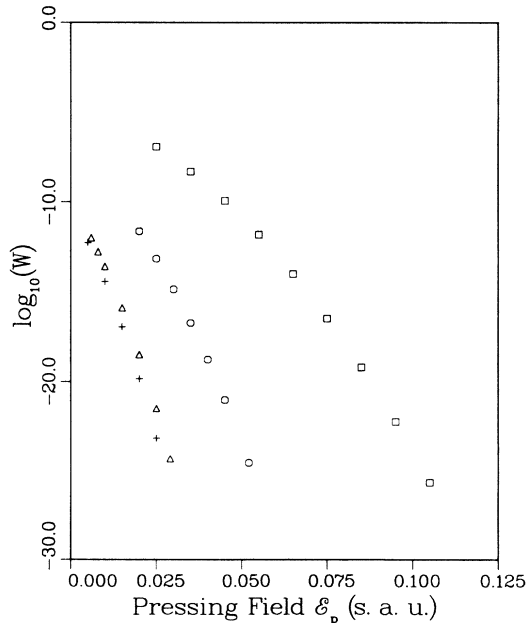


FIG. 2. External field  $\mathcal{E}_p$  dependence of tunneling rates  $W$  from the ground state.  $\mathcal{E}_c$  and  $r_0$  are ( $\circ$ ) 0.143, 34.0, ( $\square$ ) 28.0, 0.236, ( $\triangle$ ) 30.0, 0.075, (+) 0.143, 61.8, respectively.

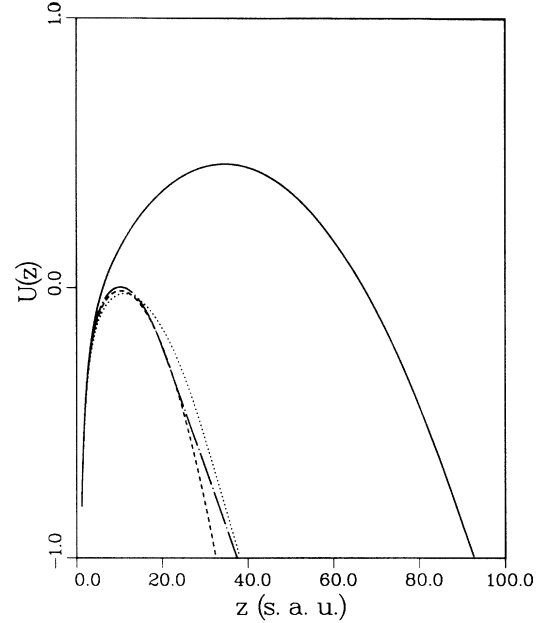


FIG. 3. The expected potential from the model of Iye *et al.* and three other potentials that will result in a tunneling rate comparable to experimentally reported rates. Each potential is obtained from correlation-hole model by changing some of the parameters.  $\mathcal{E}_c$ ,  $\mathcal{E}_p$ ,  $r_0$ ,  $W$ , and  $E$  are (solid line) 0.075, 0.029, 87.4,  $\approx 10^{-67}$ ,  $-0.47$ ; (dashed line) 0.300, 87.4, 0.026,  $4.8 \times 10^{-17}$ ,  $-0.47$ ; (dash-dotted line) 0.075, 0.029, 20.0,  $3.2 \times 10^{-17}$ ,  $-0.46$ , (dotted line) 0.075, 0.020, 30.0,  $3.3 \times 10^{-19}$ ,  $-0.47$ . The experimental rate for parameters of the solid line would be  $\approx 5.0 \times 10^{-18}$ .

it is not possible to reconcile the measured rates and activation energies with tunneling from the ground state with a static effective one-particle potential. If we abandon the correlation-hole potential and construct a barrier whose height and width are consistent with the measured thermal activation energies and escape rates, we end up with a potential whose width is 4–5 times smaller. Such a narrow potential implies that the correlation hole closes at distances much less than  $(\pi n)^{-1/2}$ . This means that, to the tunneling electron, the charge sheet already looks uniform very close to the liquid helium surface, at distances that are much smaller than the interelectronic spacing. Obviously a static charge distribution will not look uniform at such short distances when the correlations are large, as they indeed are in these experiments. For this to happen one may have to invoke some new mechanism that would introduce the dynamics of the electron sheet into the tunneling process. But this would seem difficult in view of the preponderance of low frequencies in the 2D plasmon spectrum, which give rise to very slow response times of the electron sheet compared to the characteristic tunneling times.

A simpler possibility is to consider tunneling out of excited states that, at the relatively high temperatures of the experiment, should contribute to the observed escape rates. We calculated the two lowest resonance energies

TABLE III. Correlation radius dependence of lowest two resonance energies and their widths for an experimentally studied case with  $\mathcal{E}_c = 0.143$  and  $\mathcal{E}_p = 0.052$ .  $x [y] = x \times 10^y$ .

$r_0$	$E_r$	$n=1$		$E_r$	$n=2$	
		$Q$	$W^a$		$Q$	$W$
61.8	-0.428 27	0.968 06	1.0[-46]	0.096 22	0.443 58	6.53[-26]
55.0	-0.428 63	0.898 64	1.0[-41]	0.093 22	0.376 78	4.63[-21]
50.0	-0.428 96	0.846 70	1.0[-37]	0.090 47	0.327 27	1.00[-17]
45.0	-0.429 36	0.793 72	1.0[-33]	0.087 04	0.277 31	1.34[-14]
40.0	-0.429 87	0.739 33	1.0[-28]	0.082 68	0.226 77	1.07[-11]

<sup>a</sup>Estimated by extrapolation from Fig. 1.

as a function of  $r_0$  for one value of density and field reported in the Goodkind *et al.* experiment,  $n = 2.7 \times 10^8$ ,  $\mathcal{E}_p = 91$  V/cm. The results, which also include the widths of first excited states and the estimated values for the ground state, are given in Table III. We found that the excitation energy to the second level is weakly dependent on the correlation radius and is approximately 8 K. This weak  $r_0$  dependence is due to the small contribution of  $U_c(z)$  to shifts in energy as compared to those of pressing field. The lifetimes in Table III are calculated under the assumption that electrons in the excited level remain localized laterally within a correlation disk, as if they had stayed in the 2D electron sheet. But in equilibrium the wave function of an excited electron will probably spread out and be less sensitive to the details of the distribution of the ground-state electrons. Assuming that this spreading takes much longer than the calculated lifetimes, we find that the ratio of the tunneling rate from the ground state  $W_1$ , to that from the first excited state  $W_2$  is, as listed in Table III, less than  $10^{-17}$ . In the opposite case when spreading occurs much faster than tunneling, the lifetime will be determined by how fast this delocalization takes place and the ratio  $W_1/W_2$  will be even smaller.

At finite temperatures, electrons can escape from excited states as well as from the ground state. But only the tunneling rate out of the ground state is temperature independent. Tunneling out of an excited state will appear thermally activated with an energy equal to the excitation energy. If the electrons are in thermal equilibrium, the temperature below which the tunneling from the excited states can be neglected is  $T \ll (E_2 - E_1)/\ln(W_2/W_1)$ . Thus when  $E_2 - E_1 = 8$  K and  $W_2/W_1 = 10^{17}$ , the ground-state tunneling would only be observable for temperatures below 200 mK. In the Goodkind *et al.* experiment the temperature-independent escape rates were observed around 0.5 K. If these rates are indeed due to tunneling out of the ground state, the ratio  $W_2/W_1$  must be less than  $10^7$ . Such ratio would imply a much smaller barrier than required by the activation energy. Another explanation suggests itself by examining Fig. 3 of Ref. 8, if we note that within the reported experimental error of 5%, the escape rates saturate at the same temperature of  $\approx 480$  mK for all pressing fields. The temperature-independent regime could be due to an electronic temperature that reaches its lowest limit at a slightly higher temperature than the thermometer. For example, since

the electron-rippion interaction is very weak, the electrons could easily be heated above the temperature of the helium bath with modest amounts of stay rf power.<sup>17</sup> In such a case the lowest electronic temperature attainable would be limited by the radiation leak into the cell.

We must conclude that the escape rates measured by Goodkind *et al.* cannot be due to tunneling from the ground state if correlations are taken into account by using a single-particle potential. At the relatively high temperatures of the experiment it is possible that an activated process such as tunneling out of excited states is responsible for the observed escape rates. Since the thermally activated escape rate from an excited state, in thermal equilibrium, is equal to the product of the probability of being in such a state and the escape rate from that state, activation energies will be the same regardless of the initial state. Therefore, measured activation energies do not rule out such a possibility, especially in view of the very narrow temperature ranges over which constant rates were observed.

Alternatively, a one-particle approach might be inadequate for dealing with tunneling from a strongly correlated system, in which case a more sophisticated many-body theory is needed. Along this line Azbel and Platzman<sup>18</sup> proposed a model in which local-density fluctuations in the electron sheet are responsible for the unusually large escape rates.

Thus to answer many questions arising from the discrepancy between the experiment and the calculations, both experiments and theory need to be developed. Experimentally, it would be essential to reduce the electronic temperature sufficiently so that tunneling from excited states is negligible. In addition, it would be important to develop a technique in which the electronic density is measured directly. This would avoid many uncertainties arising from the indirect capacitance measurements, such as effects of stray charges, etc. To clarify the effects of correlations, a wider range of electron densities would have to be explored. In particular, investigating the very low density regime could contribute to our understanding of the transition between the simple uncorrelated case and the correlated one. Experiments such as microwave spectroscopy of excited states could be used in selecting a realistic potential for calculating tunneling rates, since the excited states are more sensitive to details of the potential at large distances.

## ACKNOWLEDGMENTS

This work is supported by National Science Foundation (NSF) Grant No. DMR-8705977 and John von Neumann Supercomputing Center. We would like to thank J. Goodkind, P. Platzman, A. Ruckenstein, Y. Vil'k, and F. I. B. Williams for useful discussions.

## APPENDIX: NUMERICAL PROCEDURES

If the electric field of the electrons is approximated by that of a uniform charge sheet, the potential energy is

$$U(z) = -\frac{1}{z} - (\mathcal{E}_c - \mathcal{E}_p)z. \quad (\text{A1})$$

Since the external field is applied with a pair of metal plates, the potential at the electron sheet is modified as a result of the induced charges on the plates. Instead of writing this contribution explicitly we will include it in the external potential. The corresponding Schrödinger equation has two linearly independent solutions for every value of energy  $E$ . The physical solution will be described by a linear combination that gives a vanishing wave function at the origin. To find the solution we expand the wave function  $\Psi(z)$  around an arbitrary  $z_0$ ,

$$\Psi(z) = \sum_{n=0}^{\infty} \alpha_n (z - z_0)^n, \quad (\text{A2})$$

and substitute it into the Schrödinger equation to obtain a recursion relation for  $\alpha_n$ . If  $z_0 = 0$  this procedure gives only one solution, which vanishes at the origin. Since the second solution, which can be obtained from the first one, diverges at the origin it is not physical and therefore can be discarded. Around the origin the expansion coefficients  $\alpha_n$  satisfy

$$\begin{aligned} \alpha_0 &= 0, \\ \alpha_2 &= -\alpha_1, \\ \alpha_3 &= -\frac{1}{3}(E-1)\alpha_1, \end{aligned} \quad (\text{A3})$$

$$\begin{aligned} \alpha_n &= -\frac{2}{n(n-1)} [\alpha_{n-1} + E\alpha_{n-2} + (\mathcal{E}_c - \mathcal{E}_p)\alpha_{n-3} \\ &\quad + 2(\mathcal{E}_c - \mathcal{E}_p)\alpha_{n-4}], \end{aligned}$$

and around an arbitrary nonzero  $z_0$  they are given by

$$\begin{aligned} \alpha_2 &= -\frac{b}{z_0}\alpha_0, \\ \alpha_3 &= -\frac{1}{3z_0}(\alpha_2 + b\alpha_1 + a\alpha_0), \\ \alpha_n &= -\frac{2}{n(n-1)z_0} [(n-1)(n-2)\alpha_{n-1} \\ &\quad + 2b\alpha_{n-2} + 2a\alpha_{n-3}], \end{aligned} \quad (\text{A4})$$

where  $a$  and  $b$  are

$$\begin{aligned} a &= 2(\mathcal{E}_c - \mathcal{E}_p)z_0 + E, \\ b &= 1 + (\mathcal{E}_c - \mathcal{E}_p)z_0^2 + Ez_0. \end{aligned} \quad (\text{A5})$$

At large  $z$ , the solutions approach Airy functions, but because of the long range of the Coulomb interaction they cannot be fitted to a linear combination of Airy functions over a large interval. To express the asymptotic solutions in terms of Airy functions we replace the Coulomb potential by

$$U_t(z) = \begin{cases} -1/z, & z < z_t \\ \epsilon, & z \geq z_t. \end{cases} \quad (\text{A6})$$

The effect of this truncation on the energies and the lifetimes of the quasi-bound-states is negligible if  $z_t$  is large and  $\epsilon$  is properly chosen. As shown in Fig. 4 the Coulomb potential will be bracketed by the potentials defined by  $\epsilon = 0$  and  $\epsilon = -1/z_t$ , which provide upper and lower bounds for the true resonance energy and width. For this truncated Coulomb potential  $U_t(z)$ , the asymptotic form of the wave function is

$$\lim_{z \rightarrow \infty} \Psi(z) \approx \frac{B(\epsilon, z_t)}{\omega^{1/4}} \sin\left[\frac{2}{3}\omega^{3/2} + \delta(\epsilon, z_t)\right], \quad (\text{A7})$$

where

$$\omega = [2(\mathcal{E}_c - \mathcal{E}_p)]^{1/3}z - \frac{2(E - \epsilon)}{[2(\mathcal{E}_c - \mathcal{E}_p)]^{2/3}}. \quad (\text{A8})$$

The phase  $\delta(\epsilon, z_t)$  and amplitude  $B(\epsilon, z_t)$  of the wave function are given by

$$\tan\delta(\epsilon, z_t) = \frac{\lambda(\epsilon, z_t) + \beta(\epsilon, z_t)}{\lambda(\epsilon, z_t) - \beta(\epsilon, z_t)}, \quad (\text{A9})$$

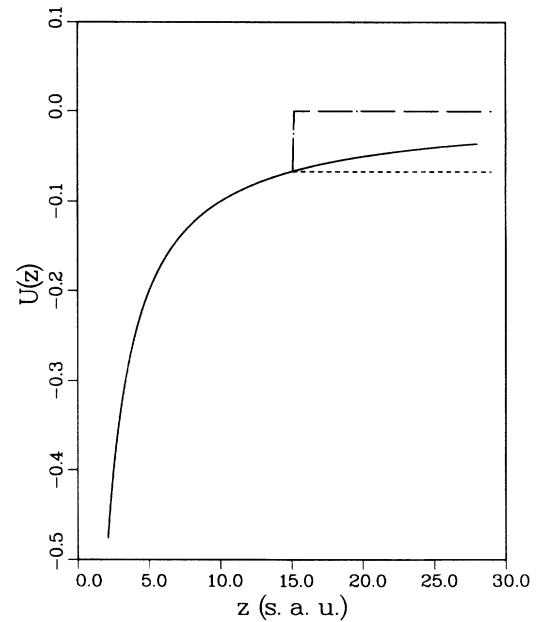


FIG. 4. Two forms of truncated Coulomb potential used in the calculations. (Solid line) Coulomb potential, (dash-dotted line)  $\epsilon = 0$ ,  $z_t = 15$ , (dashed line)  $\epsilon = -1/z_t$ ,  $z_t = 15$ . The above value of  $z_t$  is chosen for clarity. In computations it is taken to be 200 or more.

$$B(\epsilon, z_t) = \{[\lambda(\epsilon, z_t) + \beta(\epsilon, z_t)]^2 + [\lambda(\epsilon, z_t) - \beta(\epsilon, z_t)]^2\}^{1/2},$$

where for  $z \geq z_t$ ,  $\lambda(\epsilon, z_t)$  and  $\beta(\epsilon, z_t)$  are defined by

$$\Psi(z) = \lambda(\epsilon, z_t) \text{Ai}(-\omega) + \beta(\epsilon, z_t) \text{Bi}(-\omega). \quad (\text{A10})$$

For narrow resonances the phase and the amplitude will vary slowly when the energy is far from the resonance value. But in the vicinity of the resonance energy, they change rapidly and can be described by<sup>10</sup>

$$\tan[\delta(\epsilon, z_t) + \delta_0(\epsilon, z_t)] = \frac{\Gamma(\epsilon, z_t)}{2[E - E_0(\epsilon, z_t)]}, \quad (\text{A11})$$

$$B(\epsilon, z_t) = B_0(\epsilon, z_t) \left[ [E - E_0(\epsilon, z_t)]^2 + \frac{\Gamma^2(\epsilon, z_t)}{4} \right]^{1/2}.$$

In the correlation-hole model the electron contribution to potential (A1) is modified by correlations between electrons and becomes

$$U_c(z) = \begin{cases} -\mathcal{E}_c \frac{z^2}{2r_0}, & z < r_0 \\ -\mathcal{E}_c \left[ z - \frac{r_0}{2} \right], & z \geq r_0. \end{cases} \quad (\text{A12})$$

$r_0$  is given by the condition that  $g(r_0) = 0.5$ , where  $g(r)$  is the pair correlation function and  $r$  is the position of the electron in the electron sheet. In general,  $r_0$  depends on density and temperature, but for the experimentally studied regimes it is roughly given<sup>7,8</sup> by  $1.38(\pi n)^{-1/2}$ . For  $z > r_0$ , the resulting Schrödinger equation is the same as above except that the energy is replaced by  $E - \mathcal{E}_c r_0/2$ . When  $z < r_0$ , the solution around the origin is given by

$$\begin{aligned} \alpha_0 &= 0, \\ \alpha_2 &= -\alpha_1, \\ \alpha_3 &= -\frac{1}{3}(\alpha_2 + E\alpha_1), \\ \alpha_n &= -\frac{2}{n(n-1)} \left[ \alpha_{n-1} + E\alpha_{n-2} - \mathcal{E}_p \alpha_{n-3} + \frac{\mathcal{E}_c}{2r_0} \alpha_{n-4} \right], \end{aligned} \quad (\text{A13})$$

and around a general nonzero  $z_0$  it is

$$\begin{aligned} \alpha_2 &= -\frac{a}{z_0} \alpha_0, \\ \alpha_3 &= -\frac{1}{3}(\alpha_2 + a\alpha_1 + b\alpha_0), \\ \alpha_4 &= -\frac{1}{6z_0}(3\alpha_3 + a\alpha_2 + b\alpha_1 + c\alpha_0), \\ \alpha_n &= -\frac{2}{n(n-1)z_0} \left[ \frac{(n-1)(n-2)}{2} \alpha_{n-1} + a\alpha_{n-2} \right. \\ &\quad \left. + b\alpha_{n-3} + c\alpha_{n-4} + d\alpha_{n-5} \right], \end{aligned} \quad (\text{A14})$$

where  $a$ ,  $b$ ,  $c$ , and  $d$  are now given by

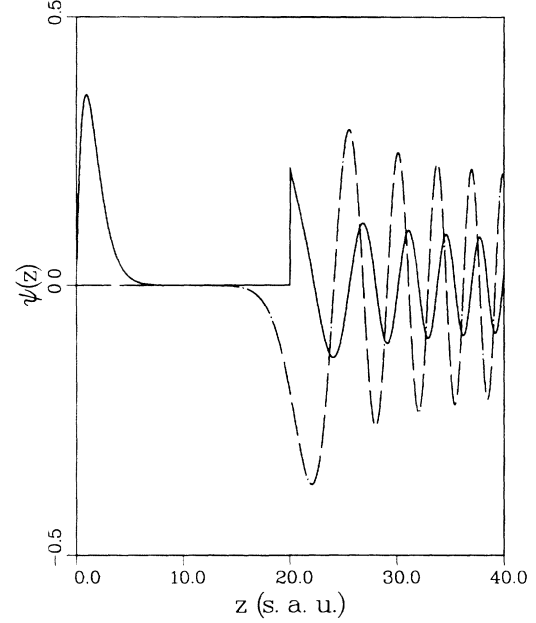


FIG. 5. Resonance (solid line) and nonresonance (dashed line) wave functions as a function of  $z$  for  $r_0 = 20$ ,  $\mathcal{E}_c = 0.236$ , and  $\mathcal{E}_p = 0.105$ . Resonance energy  $E_r$  and width are  $0.367684289351337920543$  and  $3.40 \times 10^{-17}$ , respectively. The resonance wave function is multiplied by  $5 \times 10^7$  for  $z > 20$  to show the details of the tail of the wave function. Nonresonance energy is taken to be  $E_r + 1.0 \times 10^{-5}$ . The normalization of the wave functions are chosen to bring their maximum amplitudes to comparable values.

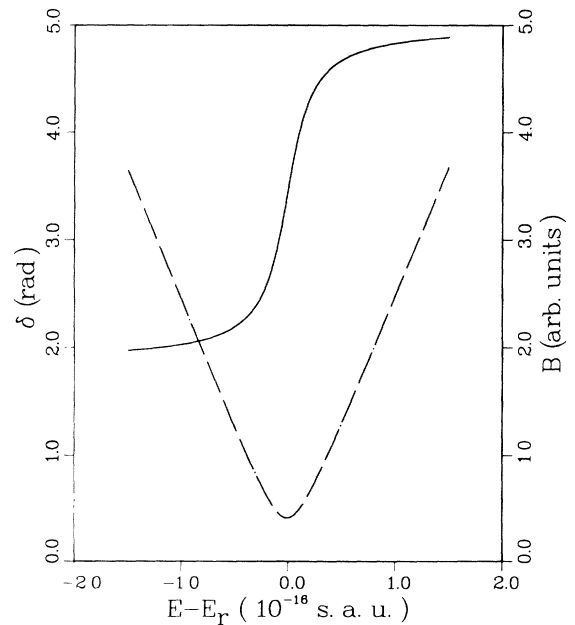


FIG. 6. Amplitude  $B$  (solid line) and phase  $\delta$  (dash-dotted line) of the resonance wave function as a function of energy around the resonance energy for the resonance parameters of Fig. 5 at  $z = z_t = 199.5$ .

$$\begin{aligned}
a &= 1 + \frac{\mathcal{E}_c z_0^3}{2r_0} - \mathcal{E}_p z_0^3 + E z_0, \\
b &= \frac{3\mathcal{E}_c}{2r_0} z_0^2 - 2\mathcal{E}_p z_0 + E, \\
c &= \frac{3\mathcal{E}_c}{2r_0} z_0 - \mathcal{E}_p, \\
d &= \frac{\mathcal{E}_c}{2r_0}.
\end{aligned}
\tag{A15}$$

The asymptotic values of the amplitude and the phase are determined from these solutions. We first calculate the wave function around the origin. Then we obtain the two linearly independent solutions around a new point  $z_0$ , beyond which the first solution cannot be determined with enough accuracy. A linear combination of these two new solutions is matched at this point to the solution around the origin. The new wave function is used to determine the solution up to a point beyond which it cannot be calculated with sufficient precision, and so on. This process is usually continued until we calculate the wave function up to a distance  $z = z_t$ , corresponding to  $\approx 200$  or more scaled atomic units, at which point we match the logarithmic derivative of the wave function to that of a linear combination of Airy functions. From the expansion coefficients, we determined the phase and the amplitude. To obtain the upper and lower bounds of the

resonance width  $W$ , we perform the calculation for  $\epsilon = 0$  and for  $\epsilon = -1/z_t$ , respectively. When  $z_t = 200$  the two limits differ by less than  $5 \times 10^{-4} W$  for almost all the calculated cases. Since both the Airy functions and the wave functions can be calculated very accurately, by this method, lifetimes as long as  $10^{30}$  can be obtained with moderate accuracy on common mainframe computers. As the uncertainty in the resonance energies is the same as that in the width, they can be determined with unprecedented accuracy. In a typical run we first detect the resonances by sudden changes in the phase. Then we determine the resonance energy  $\mathcal{E}_r$  by locating the amplitude minimum. Subsequently the energy is lowered until the phase decreases from its resonance value by  $\pi/4$  and the reduction in energy is multiplied by 2 to obtain the width. The wave function, and phase and amplitude for a typical run are shown in Figs. 5 and 6, respectively.

The activation energies are given by

$$Q = U(z_{\max}) - E_r, \tag{A16}$$

where  $z_{\max}$  is the point of maximum potential energy. When the potential energy contains the contributions due to the pressing field, the image potential, and the correlation potential  $U_c(z)$ , then, to a very good approximation

$$z_{\max} \approx \frac{\mathcal{E}_c r_0}{\mathcal{E}_p} \left[ 1 + \frac{1}{(\mathcal{E}_c r_0 / \mathcal{E}_p)^3 + 2} \right]. \tag{A17}$$

- <sup>1</sup>E. Turlot, D. Esteve, C. Urbina, J. M. Martinis, M. H. Devoret, S. Linkwitz, and H. Grabert, *Phys. Rev. Lett.* **62**, 1788 (1989).  
<sup>2</sup>G. Binning, H. Rohrer, C. Gerber, and E. Weibel, *Phys. Rev. Lett.* **49**, 57 (1982).  
<sup>3</sup>F. Capasso, K. Mohammed, and A. Y. Cho, *IEEE J. Quantum Electron.* **QE-22**, 1853 (1986).  
<sup>4</sup>M. W. Cole and M. H. Cohen, *Phys. Rev. Lett.* **23**, 1238 (1969).  
<sup>5</sup>C. C. Grimes, T. R. Brown, M. L. Burns, and C. L. Zipfel, *Phys. Rev. B* **13**, 140 (1976).  
<sup>6</sup>The scaled atomic units are the following: length  $a_B/Z = \hbar^2/(e^2 m Z) = 76.1 \text{ \AA}$ ; time  $a_B \hbar/(Z^2 e^2) = 5.0 \times 10^{-13} \text{ sec}$ ; energy  $Z^2 e^2/a_B = 15.2 \text{ K}$ ; electric field  $eZ^2/a_B = 1726.2 \text{ V/cm}$ ; and density  $Z^2 a_B^{-2} = 1.726 \times 10^{12} \text{ cm}^{-2}$ .  
<sup>7</sup>Y. Iye, K. Kono, K. Kajita, and W. Sasaki, *J. Low Temp. Phys.* **38**, 293 (1980).  
<sup>8</sup>J. M. Goodkind, G. F. Saville, A. Ruckenstein, and P. M.

- Platzman, *Phys. Rev. B* **38**, 8778 (1988).  
<sup>9</sup>R. J. Damburg and V. V. Kolosov, *J. Phys. B* **9**, 3149 (1976).  
<sup>10</sup>L. D. Landau and E. M. Lifshitz, *Quantum Mechanics, Non-Relativistic Theory* (Pergamon, Oxford, 1977), p. 555.  
<sup>11</sup>A. Maquet, S.-I. Chu, and W. P. Reinhardt, *Phys. Rev. A* **27**, 2946 (1983).  
<sup>12</sup>Y. M. Vil'k and Y. P. Monarkha, *Fiz. Nizk. Temp.* **13**, 684 (1987) [*Sov. J. Low Temp. Phys.* **13**, 392 (1987)].  
<sup>13</sup>L. D. Landau and E. M. Lifshitz, *Quantum Mechanics, Non-Relativistic Theory* (Pergamon, Oxford, 1977), p. 293, Ref. 10.  
<sup>14</sup>S. Geltman, *J. Phys. B* **11**, 3323 (1978).  
<sup>15</sup>H. Totsuji, *Phys. Rev. B* **17**, 399 (1978).  
<sup>16</sup>R. W. Hockney and T. R. Brown, *J. Phys. C* **8**, 1813 (1975).  
<sup>17</sup>D. C. Glatli, E. Y. Andrei, and F. I. B. Williams, *Phys. Rev. Lett.* **60**, 420 (1988).  
<sup>18</sup>M. Azbel and P. M. Platzman (unpublished).